JOURNAL OF SOLID STATE CHEMISTRY **126,** 195–201 (1996)
ARTICLE NO. 0329

A Crystallographic Study of the Sorption of Cadmium on Calcium Hydroxyapatites: Incidence of Cationic Vacancies

J. Jeanjean, S. McGrellis, J. C. Rouchaud, M. Fedoroff,[1] A. Rondeau, S. Perocheau, and A. Dubis

Centre National de la Recherche Scientifique, Centre d'Etudes de Chimie Métallurgique, 15 rue Georges Urbain, 94407 Vitry-sur-Seine, France

Received January 24, 1996; in revised form June 24, 1996; accepted July 10, 1996

Sorption of cadmium from aqueous solutions on several calcium hydroxyapatites was investigated as a function of pH and of the concentration of cationic vacancies, using elemental and structural analysis. The main result is that the maximum uptake of cadmium into the apatitic framework is about 0.8 mol/mol and does not depend on the stoichiometry of the starting solid. Sorbed cadium is localized in the 6*h* sites of the structure adjacent to the channels including the OH groups. For the less stoichiometric apatite (1.1 cationic vacancy per mol), the same phenomenon takes place, but a dissolution–precipitation mechanism is added, thus increasing the total quantity of cadmium immobilized in the solid. The additional sorbed quantity corresponds to the precipitation of $Cd_5H_2(PO_4)_4$. Such results may be used for the treatment of contaminated waters and industrial wastes.

INTRODUCTION

Cadmium is one of the major heavy toxic elements contaminating natural waters and industrial liquid wastes. The interaction of this element with biological apatites constituting bones leads to a disease looking like osteoporosis (1, 2). The main sources of pollution are industrial wastes and use of phosphate fertilizers. The migration in water is controlled by several equilibria between the liquid phase and solid matter, including phosphate phases. Therefore, it is of major interest to study the interaction of cadmium ions in aqueous solution with apatites and other insoluble phosphates. At the same time, use of apatites as sorbents is a promising way of eliminating cadmium from polluted waters or industrial wastes.

Previous investigations indicate that calcium hydroxyapatites are able to sorb cadmium and other heavy metal ions from aqueous solutions (2–12). Several mechanisms were proposed to explain the sorption process: superficial sorption, ion exchange, and precipitation. In our previous studies (10), we confirmed the ability of apatites to immobilize cadmium from aqueous solutions and we could localize the sites of the crystal structure of the apatite in which cadmium is sorbed. The results suggested that, under our experimental conditions, the main sorption mechanism is an ion exchange process. More recently, using measurements performed by a nuclear microprobe (13), it was shown that cadmium really diffuses into the bulk of apatite crystals, confirming that diffusion and ion exchange are the main mechanisms. A pH dependant modification of the apatite stoichiometry also takes place during sorption (14). In our experiments, the maximum uptake of cadmium which could be achieved was about 0.8 mol per mol of apatite. This concentration is far from the value expected from the number of the calcium sites available for exchange. In contrast, precipitation of cadmium–calcium hydroxyapatites leads to a continuous solid solution in which Cd/Ca ratios may vary from 0 to 1 (15).

The reason for the limitation observed in sorption experiments is still not clear. One reason may be a specificity of cadmium ions. Another reason may be connected to the possibility of diffusion in the framework of the apatite. Our previous results suggest that the diffusion takes place in the channels parallel to the *c* axis, where hydroxyl groups are located in 2*a* sites. The exchange occurs with Ca(2) cations, located in 6*h* sites adjacent to the channels (10). Vacancies may play an important role in the diffusion process. We must consider different kinds of vacancies. Vacancies of cationic sites are found in hydroxyapatites deficient in calcium. Vacancies of anionic sites are also found, especially in carbonate apatites (16, 17). The aim of the present work is to determine the eventual incidence of cationic vacancies on the limitation of the uptake of cadmium. For that purpose, a structural analysis was performed on several apatites with different cation concentrations in order to determine the vacancy concentration and distribution in the starting solids. Then, sorption of cadmium was investigated on these apatites using chemical and structural analysis.

[1] To whom correspondence should be addressed.

0022-4596/96 $18.00

EXPERIMENTAL

Materials

Four different hydroxyapatites were studied.

Three commercial synthetic calcium hydroxyapatites were used, one from Bio-Rad, referenced DNA Grade Bio-Gel HTP 130-0420, another from BDH Chemicals, referenced 44257, and the last from Merck, referenced 2196. These solids are referred to as BR, BDH, and MK, respectively. The BR and BDH powders were sieved under water flow and particles of diameter ranging from 36 to 71 μm were selected. The MK apatite was not sieved, as it is constituted of small particles of diameters less than 25 μm.

An hydroxyapatite was synthesized by mixing solutions of $Ca(NO_3)_2$ and $(NH_4)_2HPO_4$ at 70°C, the pH being stabilized at 4.5 by addition of sodium hydroxide. At such a low pH, a high cationic deficiency may be expected (18). Particles of diameter ranging from 25 to 71 μm were selected. This product is referred to as FF19.

These powders were observed by a scanning electron microscope. BR shows well-defined hexagonal-shaped crystals: the mean length along the diagonals of the crystals is 50 μm and the thickness is about 3 μm. BDH shows also hexagonal-shaped crystals with similar dimensions, but with disturbed surfaces. MK and FF19 are formed of particles with ill-defined shapes, and with very disturbed and porous surfaces. X-ray diffraction showed that BR, BDH, and MK are well crystallized. FF19 has a poorer crystallinity.

Chemical Analysis

The chemical composition of the starting hydroxyapatites and of the solutions during the sorption experiments were determined by inductively coupled plasma atomic emission spectrometry (ICP/AES), with a Thermo-Jarell-Ash Atomscan 25 sequential spectrometer.

X-Ray Diffraction

The crystal structures were determined from the diffraction line intensities collected on a step scan diffractometer fitted with a curved monochromator in the diffracted beam, a scintillation counter, and a pulse-height analyzer. Co$K\alpha$ was used with a scanning step of 0.05° 2θ in the range $15° < 2\theta < 120°$. Structure refinement was performed as already described (10) using the AFFINE (19) computer code.

Cadmium Sorption Experiments

The amount of cadmium retained in the solid and the evolution of the solid composition with pH was determined using ''batch experiments.'' Cadmium solutions of known concentration were prepared by dissolving cadmium nitrate. pH was adjusted by addition of known quantities of potassium hydroxide or nitric acid. Batches of 50 mg of hydroxyapatite were introduced into 25 ml fractions of the cadmium solutions. The starting cadmium to apatite ratio was 4 mol per mol. We have observed in a previous study (10) that a steady state is achieved after approximately 20 h. Here, the solutions with apatites were shaken at 20°C for 2 days. pH was measured again. The solutions were then filtered and analyzed for Cd, Ca, Na, K, and P by ICP/AES. The solids were characterized by X-ray diffraction.

A series of experiments was also performed under the same conditions, but without apatite, in order to control possible adsorption or precipitation effects.

RESULTS

Chemical Composition of the Starting Hydroxyapatites

The results obtained by ICP/AES showed that the four starting apatites are deficient in cations and contain sodium. For every compound two limiting formulas may be proposed (Table 1). The actual composition may be between these two formulas. This point has already been discussed (10, 14). FF19 is the most deficient in cations. It contains 1.1 cationic vacancies per unit cell. BR and BDH have close vacancy concentrations, 0.40 and 0.45, respectively. The MK apatite has a composition close to the stoichiometric value.

Crystal Structure

We have determined the crystal structure of all starting apatites. The main crystallographic parameters including the reliability factors R are given in Tables 2, 3, and 4 for apatites MK, BDH, and FF19, respectively. The crystal structure of BR has been described in a previous work (10) and the batch used here shows only slight differences to the previous one. Table 5 summarizes the cation distribution in the four compounds.

All studied apatites belong to the $P6_3/m$ space group as previously described (10). Ca^{2+} occupy two different crystallographic sites. Ca(1) is found on ternary axes at $x = 1/3$, $y = 2/3$ and Ca(2) is found at sites with symmetry m at $z = 1/4$, $z = 3/4$. In a stoichiometric apatite, Ca(1) sites are occupied by 4 atoms and Ca(2) by 6 atoms per unit cell. In MK, BR, and FF19 apatites, Ca(1) sites are entirely occupied while for BDH they are not (Table 5). For all compounds, except MK, Ca(2) sites are partially occupied, but BDH has less vacancies in this site than the other apatites. Taking into account the error intervals, the total population of Ca^{2+} (PCa(1) + PCa(2)) is in agreement with the concentrations found by ICP/AES (Table 1).

This structural study showed that these apatites are different not only by their total vacancy concentration, but

TABLE 1
Chemical Composition of the Starting Hydroxyapatites

Apatites	Limit formulas		Cationic vacancies per unit cell	Cations eq/mol
MK	$Ca_{9.8}Na_{0.06}(PO_4)_6(OH)_{1.6}$ 1.2 H_2O	(1)	0.16	19.6
	$Ca_{9.8}Na_{0.06}(PO_4)_{5.6}(HPO_4)_{0.4}(OH)_2$ 0.84 H_2O	(2)		
BR	$Ca_{9.1}Na_{0.5}(PO_4)_6(OH)_{0.7}$ 4.2 H_2O	(1)	0.40	18.7
	$Ca_{9.1}Na_{0.5}(PO_4)_{4.7}(HPO_4)_{1.3}(OH)_2$ 2.9 H_2O	(2)		
BDH	$Ca_{9.35}Na_{0.2}(PO_4)_6(OH)_{0.9}$ 2.7 H_2O	(1)	0.45	18.9
	$Ca_{9.35}Na_{0.2}(PO_4)_{4.9}(HPO_4)_{1.1}(OH)_2$ H_2O	(2)		
FF19	$Ca_{8.6}Na_{0.3}(PO_4)_{5.5}(HPO_4)_{0.5}$ 4.2 H_2O	(1)	1.1	17.5
	$Ca_{8.6}Na_{0.3}(PO_4)_{3.5}(HPO_4)_{2.5}(OH)_2$ 3.2 H_2O	(2)		

also by the distribution of vacancies between Ca(1) and Ca(2) sites.

Sorption of Cadmium

We have conducted two types of experiments: sorption of cadmium as a function of pH and sorption at nearly constant pH.

Sorption of cadmium as a function of pH. In a previous work (14) we studied the influence of pH on the sorption of cadmium ions on BR apatite. We have shown that the concentration of cadmium in the solid is almost constant, with a slight increase with pH. Here, we have studied the influence of pH for apatite MK and FF19 and completed the results for BR by increasing the pH range. Results are shown on Fig. 1. For initial pH values larger than 4, the sorbed cadmium quantities are similar in all apatites, a mean value of 0.7 mol/mol, slightly increasing with pH. It seems, however, that in the higher pH range, the most stoichiometric apatite MK leads to lower values of sorbed cadmium, but the difference is small.

For pH values between 2 and 4, the sorbed quantity is higher for FF19, about 1.8 mol/mol, while it remains at about 0.6 for MK and BR. Under pH 2, the sorbed quantity on FF19 decreases and reaches values close to 0.5, following the trend observed for pH values higher than 4 (Table 6).

Sorption of cadmium at constant pH. In order to study in more detail the influence of the stoichiometry of the apatite, the uptake of cadmium in the solid phase was measured for several concentrations of this element in the solution, with a constant initial pH value of 5, and with a contact time of 48 h. The maximum initial concentration of cadmium in the solution was 8×10^{-3} mol liter^{-1} which corresponds to 4 mol of Cd per mol of apatite. The maximum uptake of cadmium ranges between 0.7 and 0.8 mol per mol of apatite.

Structural Analysis. We have first determined the nature of the solid phases observed after cadmium sorption and then performed structure refinements on some selected samples.

In the studied pH range, sorption on MK, BR, and BDH leads to the same apatitic structure with no significant modification of the unit cell parameters. Different results were found for FF19 apatite. Large quantities of $Cd_5H_2(PO_4)_4 \cdot 4\ H_2O$ (JCPDS Tables 14-400) were found in the 2–4 pH range, where 1.8 mol of cadmium per mol of apatite is sorbed. A smaller quantity of this phase was also detected with FF19 apatite for pH values higher than 4. In this pH range, this phase was not detected for MK, BR, and BDH apatites, although the sorbed quantities are similar in all four apatites.

We have determined the crystal structures after cadmium sorption. The powder data does not show any modification of the symmetry. The main crystallographic parameters are reported in Tables 2, 3, and 4 (sample with cadmium). Results are summarized in Table 6. Taking the BDH apatite as an example, we observe that the population ($P_{Ca(2)}$ apparent) of cations that occupy Ca(2) sites (6.3) is higher than the population of Ca(2) sites in the initial sample (5.5). We must remember that structural analysis is only sensitive to the electron density; two cations of a different nature located in the same site cannot be distinguished from each other. Assigning a site to several cations was based on the chemical analysis, on the respective X-ray diffusion coefficients of Cd and Ca, and on the evolution of the population before and after sorption. So, the population of cations which effectively occupies Ca(2) sites ($P_{Ca(2)}$ real) is 0.76 Cd^{2+} + 4.5(3) Ca^{2+}. Ca(1) sites remain partially vacant,

TABLE 2

Crystallographic Data for MK Hydroxyapatite before and after Cd Sorption: Atomic Coordinates *X Y Z*, Population *P*, Occupancy Factors OF, Temperature Factors *B* (Å^2), Reliability Factor *R*, and Unit Cell Parameters *a* and *c* (Å)

		Starting sample	Sample with Cd
P	*X*	0.390(5)[a]	0.389(4)
(6*h*)	*Y*	0.363(4)	0.360(5)
	Z	1/4	1/4
	B	2.4(8)	2.7(9)
O(1)	*X*	0.323(7)	0.325(7)
(6*h*)	*Y*	0.474(7)	0.467(7)
	Z	1/4	1/4
	B	3.(1)	2.
O(2)	*X*	0.586(8)	0.585(8)
	Y	0.480(8)	0.470(9)
	Z	1/4	1/4
	B	2.(1)	2.7(9)
O(3)	*X*	0.343(5)	0.344(7)
(12*i*)	*Y*	0.255(5)	0.260(7)
	Z	0.069(3)	0.071(3)
	B	3.(1)	2.8(9)
Ca(1)	*X*	1/3	1/3
(4*f*)	*Y*	2/3	2/3
	Z	0.0014	0.0014
	B	3.4(9)	2.7(9)
	P	3.9(2)	3.9(2)
	OF	0.98	0.98
Ca(2)	*X*	0.248(3)	0.247(4)
(6*h*)	*Y*	−0.0065	−0.0065
	Z	1/4	1/4
	B	3.7(7)	2.9(8)
	P	5.8(3)	6.4(3)
	OF	0.97	1.05
OH	*X* = *Y*	0.	0.
(4*e*)	*Z*	0.18(2)	0.19(2)
	B	2.	2.
	P	2.1(3)	1.8(3)
	OF	0.52	0.45
R		0.084	0.087
a		9.415(5)	0.410(5)
c		6.879(5)	6.875(5)

[a] Standard deviation on the last digit.

with the same concentration of vacancies as before cadmium sorption. Direct calculations from intensity data without using chemical analysis gives similar distributions, but with higher errors.

These results mean that cadmium does not penetrate into Ca(1) sites, even if there are vacancies in these sites. The total population of Ca^{2+}, determined by X-ray diffraction in Ca(1) + Ca(2) sites (8.1(5) Ca^{2+}), is in agreement with the value determined by ICP/AES, taking into account the error intervals.

We have already reported (10) the crystal structure of BR after sorption of cadmium. Here also, Cd cations are located in Ca(2) sites. The same happens for MK and FF19. The population of Ca(1) sites is not modified by the sorption of cadmium. The number of vacancies

TABLE 3

Crystallographic Data for BDH Hydroxyapatite before and after Cd Sorption: Atomic Coordinates *X Y Z*, Population *P*, Occupancy Factors OF, Temperature Factors *B* (Å^2), Reliability Factor *R*, and Unit Cell Parameters *a* and *c* (Å)

		Starting sample	Sample with Cd
P	*X*	0.384(5)	0.389(5)
(6*h*)	*Y*	0.357(4)	0.362(5)
	Z	1/4	1/4
	B	2.	1.0(9)
O(1)	*X*	0.340(7)	0.334(9)
(6*h*)	*Y*	0.490(8)	0.486(9)
	Z	1/4	1/4
	B	2.	2.
O(2)	*X*	0.586(8)	0.585(9)
(6*h*)	*Y*	0.480(8)	0.470(9)
	Z	1/4	1/4
	B	2.	2.
O(3)	*X*	0.348(9)	0.352(8)
(12*i*)	*Y*	0.253(8)	0.264(8)
	Z	0.066(3)	0.066(3)
	B	2.	3.(1)
Ca(1)	*X*	1/3	1/3
(4*f*)	*Y*	2/3	2/3
	Z	0.0014	0.0014
	B	2.	2.
	P	3.5(2)	3.6(2)
	OF	0.88	0.9
Ca(2)	*X*	0.248(4)	0.247(4)
(6*h*)	*Y*	−0.0065	−0.0065
	Z	1/4	1/4
	B	1.8(9)	3.(1)
	P	5.5(3)	6.3(3)
	OF	0.92	1.03
OH	*X* = *Y*	0.	0.
(4*e*)	*Z*	0.24(4)	0.22(3)
	B	2.	2.
	P	1.7(3)	1.6(3)
	OF	0.42	0.4
R		0.089	0.087
a		9.426(5)	0.423(5)
c		6.865(5)	6.865(5)

TABLE 4

Crystallographic Data for FF19 Hydroxyapatite before and after Cd Sorption: Atomic Coordinates *X Y Z*, Population *P*, Occupancy Factors OF, Temperature Factors *B* (Å^2), Reliability Factor *R*, and Unit Cell Parameters *a* and *c* (Å)

		Starting sample	Sample with Cd
P	*X*	0.386(7)	0.384(7)
(6*h*)	*Y*	0.361(7)	0.361(6)
	Z	1/4	1/4
	B	2.	2.
O(1)	*X*	0.340(9)	0.340(8)
(6*h*)	*Y*	0.499(9)	0.490(8)
	Z	1/4	1/4
	B	2.	2.
O(2)	*X*	0.587(9)	0.583(8)
(6*h*)	*Y*	0.482(9)	0.475(8)
	Z	1/4	1/4
	B	2.	2.
O(3)	*X*	0.356(7)	0.349(7)
(12*i*)	*Y*	0.264(8)	0.264(6)
	Z	0.074(4)	0.065(4)
	B	2.	2.
Ca(1)	*X*	1/3	1/3
(4*f*)	*Y*	2/3	2/3
	Z	0.0014	0.0014
	B	3.(1)	4.(1)
	P	4.0(2)	3.8(2)
	OF	1.	0.95
Ca(2)	*X*	0.248(4)	0.250(4)
(6*h*)	*Y*	−0.0065	−0.0065
	Z	1/4	1/4
	B	3.(1)	3.(1)
	P	4.8(3)	5.6(3)
	OF	0.80	0.93
OH	*X* = *Y*	0.	0.
(4*e*)	*Z*	0.20(2)	0.19(2)
	B	2.	2.
	P	1.9(3)	1.8(3)
	OF	0.48	0.45
R		0.091	0.088
a		9.435(5)	9.445(5)
c		6.865(5)	6.855(5)

in Ca(2) sites remains almost unaffected, or slightly increases.

DISCUSSION

As already pointed out, we did not observe any significant variation of cell parameters of the apatitic phase after cadmium fixation. In mixed calcium–cadmium hydroxyapatites prepared by coprecipitation (15), a decrease of the unit cell parameters is observed as the Cd/Ca ratio increases in the solid. From these results, it appears that a 0.8 mol/mol Cd concentration is too small to induce a significant modification of cell parameters.

TABLE 5

Crystallographic Data for Starting Hydroxyapatites: MK, BR, BDH, and FF19: Cationic Population ($P_{Ca(1)}$ and $P_{Ca(2)}$), Number of Vacancies in Ca(2) Sites ($V_{Ca(2)}$), and Unit Cell Parameters

	MK	BR	BDH	FF19
$P_{Ca(1)}$	3.9(2)	3.7(2)	3.5(2)	4.0(2)
$P_{Ca(2)}$	5.8(3)	5.3(3)	5.5(3)	4.8(3)
$V_{Ca(2)}$	0.2(3)	0.7(3)	0.5(3)	1.2(3)
a(Å)	9.415(5)	9.436(5)	9.426(5)	9.435(5)
c(Å)	6.879(5)	6.880(5)	6.865(5)	6.865(5)

Concerning the sorption mechanisms, the results suggest two possible processes. For MK, BR, and BDH apatites, which have the smallest concentration of cationic vacancies (<0.5 vacancy per unit cell), sorption proceeds by incorporation of cadmium into the apatitic structure, more precisely into the Ca(2) sites. This process takes place in a large pH range. Several complementary results indicated that the most likely incorporation process is diffusion and ion-exchange. Scanning electron microscope observations showed that there is no modification of the crystallite morphology after cadmium fixation. More recently, nuclear microprobe measurements showed that cadmium has penetrated into the whole thickness of the crystals (13).

The exchange occurs exclusively with Ca(2) sites adja-

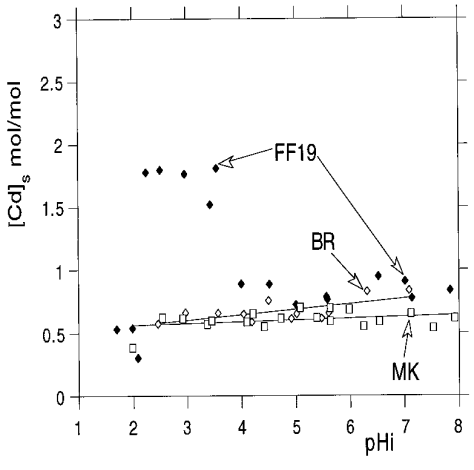

FIG. 1. Variation of the sorbed concentration of cadmium $[Cd]_s$ in three calcium hydroxyapatites (MK, BR, and FF19) with different cationic vacancy concentrations as a function of initial pH. See compositions and vacancy concentrations in Tables 1 and 5.

TABLE 6
Composition Determined by Chemical Analysis, Cationic Population per Unit Cell Determined from X-Ray Diffraction for MK, BDH, and FF19 Apatites with Cadmium

	MK	BDH	FF19
Chemical analysis	$Cd_{0.70}Ca_{9.24}$-HA	$Cd_{0.76}Ca_{8.65}$-HA	$Cd_{0.73}Ca_{7.84}$-HA
$P_{Ca(1)}$	3.9(2) Ca^{2+}	3.6(2) Ca^{2+}	3.8(2) Ca^{2+}
$P_{Ca(2)}$ apparent	6.4(3) Ca^{2+}	6.3(3) Ca^{2+}	5.6(3) Ca^{2+}
$P_{Ca(2)}$ real	0.70 Cd^{2+} + 4.7(3) Ca^{2+}	0.76 Cd^{2+} + 4.5(3) Ca^{2+}	0.73 Cd^{2+} + 3.9(3) Ca^{2+}
$(Ca)_{total}$	8.6(5) Ca^{2+}	8.1(5) Ca^{2+}	7.9(5) Ca^{2+}

cent to the channels centered on the hexagonal screw axes and containing the OH ions. These results may be compared to those obtained by Nounah *et al.* (20) using a cadmium–calcium hydroxyapatite obtained by precipitation. In this last case, cadmium is found in both Ca(1) and Ca(2) sites, although with an unequal distribution. This was discussed with respect to the ionic radii and bond strengths. Thus, with the same cation, sorption, and precipitation do not lead to the same site occupancy. This difference probably results from the fact that, during sorption, cadmium diffuses in the channels and has direct access to Ca(2) sites adjacent to them. An interesting feature of BDH apatite is the partial occupancy of Ca(1) sites. The partial occupancy of these sites remains after sorption, indicating that cadmium has no access to these sites, which are not directly connected to the channels.

In the case of FF19, the least stoichiometric apatite studied in this work, diffusion into the apatitic framework also takes place, as indicated by the structural analysis of the apatitic phase. In this case, a second process occurs, as indicated by the advent of the $Cd_5H_2(PO_4)_4 \cdot 4\,H_2O$ phase. This is probably a dissolution–precipitation mechanism. This mechanism plays a major role in the pH 2–4 range and has the advantage of increasing the total quantity of cadmium immobilized in the solid phase (1.8 mol per mol). It plays a minor role in FF19 for higher pH values, while it was not detected at all for more stoichiometric apatites.

Concerning the apatitic phase, this work confirmed that the maximum cadmium concentration achieved under our experimental conditions is about 0.8 mol per mol. This limitation is not dependent on the number of cationic vacancies in Ca(2) sites, nor on the distribution of vacancies between Ca(1) and Ca(2) sites. It should however be noticed that in the four investigated hydroxyapatites the occupancy of channels by hydroxyl groups or water is similar (10). It will be interesting to study apatites with less occupied channels, such as carbonato-apatites (16, 17).

An unexpected result is that the less stoichiometric apatite (FF19) induced a dissolution–precipitation process. This result may be explained by the instability of such apatites, leading to larger dissolution and, therefore, to precipitation.

CONCLUSION

The first contribution of this work was to improve the knowledge of the structure of nonstoichiometric calcium hydroxyapatites. Nonstoichiometry may result from different distributions of vacancies between Ca(1) and Ca(2) sites.

This work has also improved our knowledge of the sorption mechanisms. The cationic vacancies (in the range studied) do not seem to have an influence on the maximum uptake of this element into the apatitic phase. The reason for this limitation is still not well understood and may be an intrinsic property of cadmium ions, not to occupy neighboring sites. This hypothesis may be compared to the results obtained during the superficial sorption on ferric oxides: cadmium ions never lead to multinuclear surface species (21). However, our results have shown that the use of calcium hydroxyapatites with a high cationic vacancy concentration increase the quantity of cadmium immobilized in the solid phase, due to a dissolution–precipitation process. This may be an advantage in the application of apatites for the removal of toxic metallic ions from industrial liquid wastes or from contaminated soils. The advantage of sorption over precipitation is the possibility of using a continuous process and of applying it to very low concentrations of cadmium in solution.

A listing of the observed and calculated structure factors is available on request.

REFERENCES

1. T. Miyahara, M. Miyakoshi, Y. Saito, and H. Kozuka, *Toxicol. Appl. Pharmacol.* **55,** 477 (1980).
2. J. Christoffersen, M. R. Christoffersen, R. Larsen, E. Rostrup, P. Tingsgaard, O. Andersen, and P. Grandjean, *Calcif. Tissue Int.* **42,** 331 (1988).
3. N. Nayak and B. V. C. Rao, *J. Indian Chem. Soc.* **53,** 630 (1976).
4. T. Suzuki, T. Hatsushika and Y. Hayakawa, *J. Chem. Soc. Faraday Trans. I* **77,** 1059 (1981).
5. Y. Takeuchi and H. Arai, *J. Chem. Eng. Jpn.* **23,** 75 (1990).
6. T. Suzuki, T. Hatsushika and M. Miyake, "New Development in Ion Exchange, Tokyo, Japon, 2–4 October, 1991." p. 401.
7. J. J. Middelburg and R. N. J. Comans, *Chem. Geol.* **90,** 45 (1991).
9. Q. Y. Ma, S. J. Traina, T. J. Logan, and J. A. Ryan, *Environ. Sci. Technol.* **27,** 1803 (1993).

10. U. Vincent, J. Jeanjean, and M. Fedoroff, *J. Solid State Chem.* **108,** 68 (1994).
11. Y. Xu, F. W. Schwartz, and S. J. Traina, *Environ. Sci. Technol.* **28,** 1472, (1994).
12. S. Mandjiny, A. I. Zouboulis, and K. A. Matis, *Separ. Sci. Technol.* **30**(15), 2963 (1995).
13. N. Toulhoat, V. Potocek, C. Neskovic, M. Fedoroff, J. Jeanjean, and U. Vincent, ''7th Intern. Conf. on Particle Induced X-ray Emission and its Analytical Application, Padua, Italy, May 26–30, 1995.''
14. J. Jeanjean, M. Fedoroff, F. Faverjon, U. Vincent, and J. Corset, *J. Mater. Sci.* **31,** 6156 (1996).
15. A. Nounah, J. Szilagyl, and L. Lacout, *Ann. Chim. Fr.* **15,** 409 (1990).
16. G. Bonnel, *Ann. Chim. Fr.* **7,** 65 (1972).
17. G. Bonnel, *Ann. Chim. Fr.* **7,** 127 (1972).
18. E. E. Berry, *J. Inorg. Nucl. Chem.* **29,** 1585 (1967).
19. W. R. Busing, K. O. Martin, and H. A. Levy, ''A Cristallographic Least Square Program ORFLS AFFINE.'' 1984.
20. A. Nounah, J. L. Lacout, and J. M. Savariault, *J. Alloys Compounds* **188,** 141 (1992).
21. L. Spadini, A. Manceau, P. W. Schindler, and L. Charlet, *J. Colloid Interface Sci.* **168,** 73 (1994).